Measurement of the intermolecular vibration–rotation tunneling spectrum of the ammonia dimer by tunable far infrared laser spectroscopy

M. Havenith,[a] R. C. Cohen, K. L. Busarow, D-H. Gwo, Y. T. Lee, and R. J. Saykally
Department of Chemistry, University of California, and Materials and Chemical Sciences Division, Lawrence Berkeley Laboratory Berkeley, California 94720

(Received 25 October 1990; accepted 20 December 1990)

Over 150 lines in six tunneling subbands of an intermolecular vibration located near 25 cm^{-1} have been measured with partial hyperfine resolution and assigned to $(NH_3)_2$. The transitions sample all three types of tunneling states (A, G, E) and are consistent with the following assumptions: (1) G_{36} is the appropriate molecular symmetry group; (2) the equilibrium structure contains a plane of symmetry; (3) interchange tunneling of inequivalent monomers occurs via a *trans* path; (4) the $2C_3 + I$ limit of hydrogen exchange tunneling is appropriate; (5) tunneling and rotational motions are separable. A qualitative vibration–rotation tunneling energy level diagram is presented. Strong perturbations are observed among the states of E symmetry. This work supports the conclusions of Nelson *et al.* [J. Chem. Phys. **87**, 6365 (1987)].

I. INTRODUCTION

The measurement of high resolution infrared, microwave, and far-infrared spectra of weakly bound hydride complexes has provided fundamental insight into the interesting and important concerted hydrogen tunneling dynamics that occur in these systems. Detailed investigations of $(HF)_2$,[1] $(HCl)_2$,[2] and $(H_2O)_2$,[3] have established the dimer structures, the nature of tunneling paths between equivalent structures, the classes of motion that occur, the energy level diagrams associated with the rotational and tunneling motions, and qualitative features of the intermolecular potential surfaces. Despite the intrinsic interest in these systems and phenomena, the most exciting aspect of these studies lies, nevertheless, in the extension to larger clusters and in the corresponding prospects for elucidating the complex nature of local motions that occur in hydrogen bonded liquids and solids. Such knowledge seems essential for reliable modeling of proton transfer in these environments—a feat which remains beyond the means of current theories and theoreticians.

The ammonia dimer has proven to be an unexpectedly interesting and controversial object of these studies.[4] Although ammonia has for many years served as a prototypical example of the traditional view of a hydrogen bonding system (both as donor and acceptor), recent investigations by Klemperer and co-workers[4–6] have shown that ammonia surprisingly does not act as a proton donor in any of its known binary complexes. In particular, the equilibrium structure of $(NH_3)_2$ characterized by Nelson *et al.*[5,6] does not exhibit the expected near-linear hydrogen bonds. Rather, the C_3 axes of the monomers are offset and oriented nearly antiparallel, but making inequivalent angles (49° and 115°) with the a inertial axis of the complex. This type of structure has been reproduced in only one high level *ab initio* calculation,[7] whereas many others[8–16] produce the traditional linearly hydrogen bonded form. Furthermore, the experimental structure is not consistent with results from electrostatic models for the attractive potential.[17]

The structure obtained by Nelson *et al.*[5,6] was deduced from precise microwave measurements of two pure rotational transitions in $K_a = 0$ ($J = 1 \leftarrow 0$ and $J = 2 \leftarrow 1$) in two tunneling states (G_α and G_β) for several isotopic forms of the dimer. Because the observed transitions appeared to be pure rotational transitions, it was concluded that they did not involve a change in tunneling state, and could thus directly characterize the dimer structure. The structural information was contained in the effective rotational constants, dipole moments, and quadrupole coupling constants. The first of these yields the vibrationally averaged distance between the monomer centers of mass, while the latter two provide vibrationally averaged angles between the monomer C_3 axes and the inertial axes of the complex. Because these angles did not vary significantly with isotopic substitution, it was concluded that the effective ("zero-point") structures obtained were reliable approximations to the equilibrium structure. Nevertheless, the disagreement between the theoretical structures and that obtained by Nelson *et al.* has been attributed to vibrational averaging effects in recent papers describing more detailed theoretical calculations.[17,18] New calculations by Dykstra[19] employing an electrostatic model with *ab initio* values for the molecular properties do actually produce a structure that is fairly close to that of Nelson *et al*; one can rationalize this structure as resulting from the nitrogen lone pairs interacting simultaneously with *two* hydrogens. However, the level of agreement is still unsatisfactory. Considering the central importance of the ammonia dimer as a paradigm for hydrogen bonding, this discrepancy needs to be resolved.

The concerted hydrogen tunneling dynamics occurring in $(NH_3)_2$ were characterized by Nelson and Klemperer[20] using dynamical group theory. The microwave transitions could be explained using the permutation–inversion group

[a] Institut für Angewandte Physik, der Universität Bonn, Wegelerstrasse 8, D-5300 Bonn 1, West Germany.

 0021-9606/91/074776-14$03.00

G_{36}. Each rotational level is split into eight tunneling levels: two A states, two G states, and four E states. In the free rotor limit, these states correspond to different combinations of internally rotating monomers. For A states, both monomers have zero quanta of internal rotation about their C_3 axes ($m = 0$). In G states, only one monomer is rotating ($m = 1$), whereas in E states both monomers have $m = 1$. The G states are distinguished from other states because they follow different selection rules; they are the only states for which a-type pure rotational transitions are allowed. The interchange tunneling, which exchanges the inequivalent monomers, is quenched in the G states because the two different internal rotational quanta ($m = 0$ and $m = 1$) for the two monomers correspond to different nuclear spins. Thus, an interchange would imply an exchange of nuclear spin.

The microwave measurements of Nelson *et al.*[5,6] sampled *only* the G states. Measurements of the ν_2 umbrella vibration in the infrared, reported by several groups,[21-23] were unable to resolve either the different tunneling or rotational states, due to line broadening from rapid predissociation. Hence, neither the A nor E states have been characterized previously. In this paper we report the measurement of hyperfine-resolved far infrared intermolecular vibration–rotation tunneling (VRT) spectra of $(NH_3)_2$ in which *all* classes of tunneling states are sampled. An analysis is presented which supports the conclusions reached by Nelson *et al.*, and which suggests a qualitative VRT energy level diagram for the system.

II. EXPERIMENTAL

VRT spectra were observed with the Berkeley tunable far infrared (FIR) laser spectrometer, which has been described previously.[24-26] The $Ar_n(NH_3)_m$ clusters were produced in a continuous, two-dimensional supersonic jet.[27] Typical conditions involved expanding a mixture of 3% NH_3 in argon at approximately 1 atm through a 3.7 cm$\times$25 μm slit into a chamber maintained at 100 mTorr by an 1800 cfm Roots blower pumping system. Tunable FIR radiation was generated by mixing a fixed frequency FIR laser with tunable microwave radiation (2–42 GHz and 48–70 GHz) in a Schottky barrier diode. Nearly continuous scanning was performed with the 432 and 394 μm (692.9513 and 761.6083 GHz) formic acid laser lines. In addition, some spectra were measured using the 513 μm (584.3882 GHz) formic acid line. Both sidebands (sum and difference frequency) were detected simultaneously. Spectra were recorded using frequency modulation of the microwave source and lock-in detection at $2f$ with an InSb hot electron bolometer. The linewidths are determined by the residual Doppler broadening of 400 kHz (FWHM). This is sufficiently narrow to enable the partial resolution of quadrupole hyperfine structure in $(NH_3)_2$. The laser was frequency-pulled during the measurements in order to determine if the transition was due to absorption of the lower or upper sideband, and then set back to the maximum power. This procedure results in small frequency deviations, which along with thermal drift in the cavity length, limit the accuracy in the frequency measurements to approximately 1 MHz.

Using the argon/ammonia mixture, more than 300 absorption lines were measured over the range from 21 to 28 cm^{-1} (625 to 830 GHz), as shown in Fig. 1. Twenty-three of the strongest lines could be assigned to transitions from $ArNH_3$,[28] and about 150 were assigned to $(NH_3)_2$. The strongest lines of $(NH_3)_2$ exhibited a signal-to-noise ratio of about 100, whereas those assigned to $ArNH_3$ were twice as strong.

III. THEORY

A. Group theoretical considerations

Nelson *et al.*[5,6,20] have argued that the most appropriate molecular symmetry group for $(NH_3)_2$ is the group G_{36}. Larger symmetry groups are only required if the inversion tunneling of each monomer is active. NH_3 inversion has been shown to be quenched in all NH_3-containing complexes studied to date except Ar–NH_3,[29,30] and it appears reasonable to assume that it is quenched in the NH_3 dimer until evidence suggests otherwise. The operations which make up the G_{36} group are generated from C_3 rotations about the monomer axes, interchange of the two NH_3 monomers, and inversion of all particle coordinates in the center of mass multiplied by an appropriate permutation of nuclei to conserve the handedness of each monomer. Nelson *et al.*[20] predicted that eight tunneling sublevels of each vibration–rotation level should be present if G_{36} is the appropriate symmetry group and assuming that the equilibrium structure possesses a plane of symmetry. They also assumed this molecular plane to contain the a and b inertial axes of the complex, although they note that it could equally well be the $a + c$ plane. Only two sets of pure rotation transitions were predicted to occur among these eight sublevels. This is consistent with the spectra observed by MBER, and constitutes experimental evidence, albeit negative, for G_{36} being the appropriate molecular symmetry group.

Although they were able to observe only the two sets of pure rotational transitions in the tunneling states with vibration–tunneling symmetry G (throughout this work we use italic type to indicate vibration–tunneling symmetry and ordinary print to indicate symmetry labels referring to the full

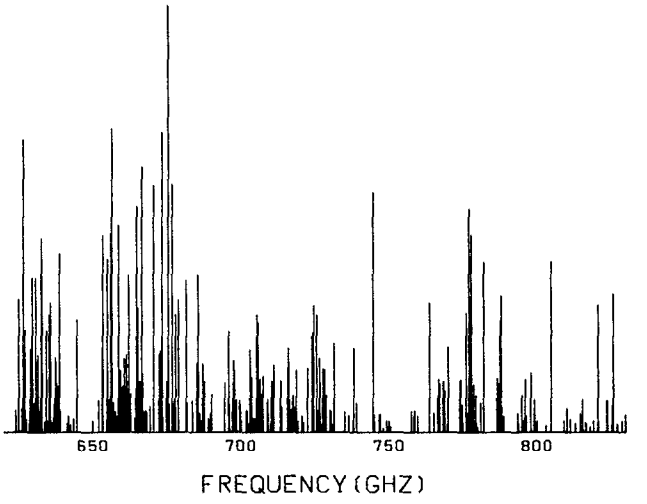

FIG. 1. 300 absorption lines measured over the range of 21 to 28 cm^{-1}.

VRT state), Nelson and Klemperer[20] established a theoretical correlation diagram which gives an indication of the size of the various tunneling splittings and the proposed energy level ordering. In doing so, they made use of group theoretical arguments and analogies to the more thoroughly studied $(HF)_2$ and $(H_2O)_2$ systems.[1,3] They concluded that the most likely situation is one in which hindered C_3 rotations leading to permutations of the hydrogen nuclei are especially facile, with the second motion—the interchange of the inequivalent NH_3 subunits within the complex—being somewhat more hindered. This limit, denoted $(2C_3 + I)$, implies that the hydrogen exchange tunneling frequency associated with C_3 rotation about the C_{3v} axis of each of the two monomers is higher than the interchange frequency, and therefore that the tunneling splitting associated with hindered rotation is larger than the interchange tunneling splitting. Several other limiting cases were considered, viz., $(I + 2C_3)$, $(2C_3)$, (I). Consideration of the selection rules prevailing in each case provides the strongest evidence for the $(2C_3 + I)$ limit. For this case, *only* pure rotational transitions are allowed for the two G states. In the $(I + 2C_3)$ limit, only tunneling–rotational transitions are allowed. Nelson *et al.* observed only the former situation.

Assuming that G_{36} is the correct molecular symmetry group, and that the rigid nontunneling structure can be classified in the C_s group, we expect each rotational level of $(NH_3)_2$ to split into eight tunneling sublevels. One can qualitatively describe the tunneling motions occurring in each state by considering the correlation diagram presented by Nelson and Klemperer.[20] They show that the lowest energy levels are of A symmetry, constructed from two NH_3 monomers with each in its ground $(m = 0)$ internal rotational state. C_3 tunneling does not occur in these levels, but the two different A states (A_1 and A_4) are split by the interchange tunneling. The next lowest levels are the two G states, which are constructed from one rotating $(m = 1)$ and one nonrotating $(m = 0)$ NH_3 monomer. Because of the difficulty of exchanging different nuclear spin states ($m = 0$ is ortho, $m = 1$ is para) interchange tunneling is quenched in the G states. The two different sublevels (G_α and G_β) correspond to $NH_3(1)$ with $m = 1$ and $NH_3(2)$ with $m = 0$ and $NH_3(1)$ with $(m = 0)$ and $NH_3(2)$ with $m = 1$. The labels α and β are chosen to be consistent with the notation of Nelson *et al.* and do not reflect any fundamental molecular symmetry. In the E sublevels, both NH_3 monomers are in the $m = 1$ state. The angular momentum of the monomer rotation can be arranged in a parallel or antiparallel fashion, and interchange is again possible, since both NH_3 subunits have the same nuclear spin. Four tunneling states result: E_1, E_2, E_3, and E_4.

B. Selection rules

In addition to establishing a model for the VRT energy level ordering, Nelson and Klemperer[20] also give detailed consideration to the selection rules and spin statistics appropriate for $K = 0$ levels. In this section, we briefly review their results with specific reference to those points which are most relevant to the study of the intermolecular vibrations. We have expanded their treatment to include $K_a \neq 0$ levels in order to include our own measurements, which span a number of sublevels with $K_a = 1$. In Fig. 2 we show the ordering of the tunneling levels expected for $K_a = 0$ and 1 in the ground vibrational level, along with the spin statistical weights associated with each VRT level. The switch in ordering of the tunneling sublevels that is shown in $K_a = 1$ is consistent with our data, but is not rigorously confirmed at this point. The overall selection rules for VRT transitions are summarized in Table I.

VRT selection rules for perpendicular (b- or c-type) transitions may be different from a-type selection rules, and are explicitly dependent on the symmetry of the interchange tunneling path, as well as on the labeling of the axes contained in the plane of symmetry. (The plane of symmetry may contain the $a + b$ axes or the $a + c$ axes, as noted above.) Following Hougen and Ohashi[31] we distinguish between two such tunneling paths. They interpreted the $(HF)_2$ spectra using selection rules determined from considering two tunneling paths, viz. *cis* and *trans*. A diagram illustrating these two corresponding paths for $(NH_3)_2$ is given in Fig. 3. The z axis points from N_1 to N_2, the x axis is chosen to be along the b axis, which is assumed here to be in the plane of symmetry, and y points along the c axis. These two paths are the simplest to consider because of the existence of intermediate C_{2y} or C_{2x} symmetry axes. In general, a more complicated path, similar to the geared-type rotation in $(H_2O)_2$ described by Coudert and Hougen,[32] can occur. However, because there is no need at this point to consider such complications, we will restrict ourselves in the following discussion to the two paths mentioned above. The *trans* path has an intermediate C_{2y} symmetry, while the *cis* path has C_{2x} symmetry, as shown in Fig. 3. The point group operations in the C_{2y} and C_{2x} groups which correspond to the operations in the permutation inversion group G_{36} are given in Table II (A). The symmetry species of the rotational wave functions, as deduced from this table, are listed in Table II (B). The symmetry of the interchange tunneling path does not affect states with even K_a. However, perpendicular b-type or c-type transitions, such as those observed here with $K_a = 1 \leftarrow K_a = 0$, obey different selection rules for the *cis* and *trans* paths because the path symmetry affects that of the

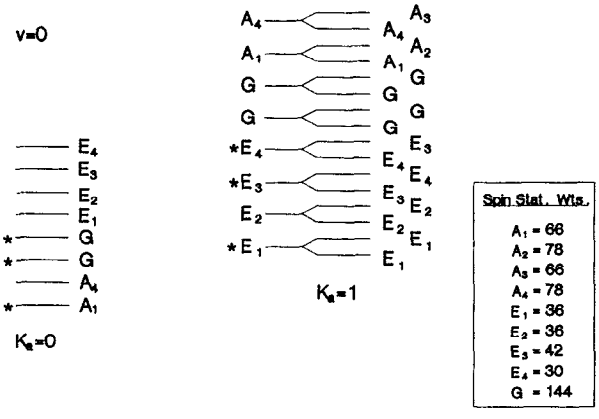

FIG. 2. Ordering of the tunneling levels expected for $K_a = 0$ and 1 in the ground vibrational level along with the spin statistical weights.

TABLE I. Overall selection rules in the G_{36} group.

$A_1 \leftrightarrow A_3$
$A_2 \leftrightarrow A_4$
$G \leftrightarrow G$
$E_1 \leftrightarrow E_2$
$E_3 \leftrightarrow E_3$
$E_4 \leftrightarrow E_4$

$K_a = 1$ level. For the *cis* path, all such transitions obey pure rotational selection rules, i.e., they do not change the tunneling sublevel. For the *trans* path, all $\Delta K = \pm 1$ transitions, except those involving the G states, require a change of vibration-tunneling state. If the c axis is contained in the plane of symmetry, then some of the path dependent selection rules change; viz, the symmetries for $K_a =$ odd states change, while those for $K_a =$ even remain the same. The rotational symmetries corresponding to this possibility are given in Table II (C) and the selection rules can be derived from them.

We shall introduce one further assumption, viz. that overall rotation can be separated from the vibrational and tunneling motions. In this case, the overall wave function can be written as a product of vibrational tunneling and rotational wave functions. Selection rules must then be derived separately for the vibration tunneling and for the rotational part of the wave function. We therefore consider separately

TABLE II. (A) Point group operations of the C_{2h} and C_{2v} point group (for *trans* and *cis* path) corresponding to elements in the permutation inversion group G_{36}. (B) Symmetry species of rotational wave functions for *cis* and *trans* paths, assuming symmetry plane contains the b axis. (C) Symmetry species of rotational wave functions for *cis* and *trans* paths, assuming symmetry plane contains the c axis.

(A)	Group G_{36}	*trans* path	*cis* path
	C_{2x}	(14)(25)(36)(78)	C_{2y}
	$\sigma(x,z)$	(23) (56)*	$\sigma(x,z)$
	C_{2x}	(142536)(78)	C_{2y}
	$\sigma(x,y)$	(14)(25)(36)(78)*	i

(B)	K_a	K_c	Γ_{rot} *trans*	Γ_{rot} *cis*
	e	e	A_1	A_1
	e	o	A_2	A_2
	o	e	A_1	A_4
	o	o	A_2	A_3

(C)	K_a	K_c	Γ_{rot} *trans*	Γ_{rot} *cis*
	e	e	A_1	A_1
	e	o	A_2	A_2
	o	e	A_2	A_3
	o	o	A_1	A_4

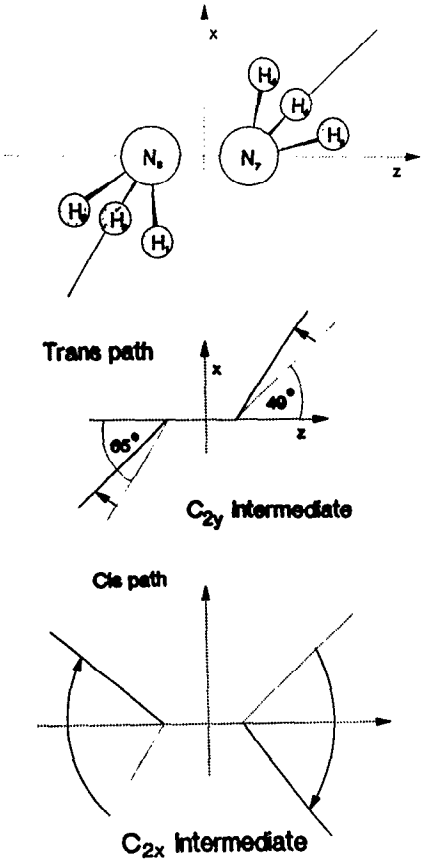

FIG. 3. The *cis* and *trans* interchange tunneling paths for $(NH_3)_2$.

the question of whether a given vibrational tunneling transition is allowed, from that of whether a given rotational transition within a vibration tunneling subband is allowed. For example, as can be seen in Fig. 2, for $K_a = 1$ there are two levels of E_3 symmetry associated with each rotational level; one is associated with the E_3 tunneling state and the other with the E_4 tunneling state. If overall rotation and internal motions were strongly coupled, then we would expect allowed transitions from either of the $J = 1$ E_3 levels to *both* of the E_3 levels in $J = 2$. On the other hand, and we will proceed here with all further discussion based on this assumption, if these two types of motion are decoupled, then the transitions from $J = 1$ in the E_3 tunneling state to $J = 2$ in the E_4 tunneling state are forbidden, and only the transition $J = 2$ $E_3(E_3) \leftarrow J = 1 E_3(E_3)$ is allowed. This situation is also depicted in Fig. 4, specifically for the case of a VRT transition.

For $K_a = 1$, both asymmetry doublets associated with the vibration tunneling state of E_1 symmetry have the same symmetry species in the group G_{36}. This is also true for the E_2 state. Thus, all four transitions among a pair of asymmetry doublets in the $E_2 \leftarrow E_1$ bands are potentially allowed. If we separate the overall rotation from the vibration tunneling motion, however, only two of the four possible transitions [either two nontunneling transitions (VR) or two tunneling (VRT) transitions] will be allowed, which is actually what was observed in the present study.

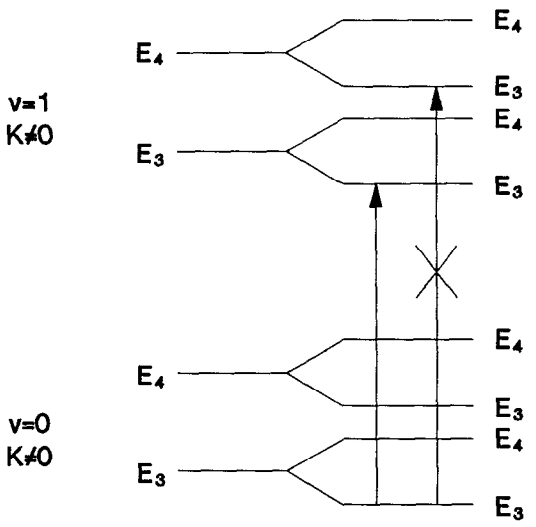

FIG. 4. For $K_a = 0$ there are two levels of E_3 symmetry associated with each rotational level: one is associated with E_3, the other with E_4.

The overall selection rules for vibration–rotation tunneling transitions also depend on the choice of the symmetry species of the vibrational states in the group G_{36}. Multiplying the wave function of the excited vibrational state RT levels by a vibrational wave function of A_3 symmetry results in all allowed transitions corresponding to nontunneling transitions, independent of which limit [$(I + 2C_3)$ or $(2C_3 + I)$] is used. On the other hand, an A_2 vibration, for example, simply induces a switch in the symmetries of the rotational wave functions, thus not changing the tunneling selection rules. The latter case is in agreement with our measurements.

C. Statistical weights

The statistical weights for each overall (VRT) symmetry species have been tabulated previously,[20] and we reproduce this table here (Table III) for convenience. Intensity patterns observed for $K_a = 1$ transitions, which result from nuclear spin statistical alternations, have been an important clue to assignment of the observed transitions. As shown in Fig. 2, intensity alternation is expected within the K-type doublets of tunneling levels with A_1, A_2, A_3, A_4, E_3, and E_4 symmetries. For the G states and the E_1 and E_2 states, no such alternation will be observed. The intensity alternation in A state K-type doublets will be 1.2:1, while in the K-type doublets of the E_3 and E_4 states it will be 1.4:1 These ratios

TABLE III. Statistical weights.

$A_1 = 66$
$A_2 = 78$
$A_3 = 66$
$A_4 = 78$
$E_1 = 36$
$E_2 = 36$
$E_3 = 42$
$E_4 = 30$
$G = 144$

are similar enough to make distinguishing between the two possibilities very difficult, given the signal/noise ratio of the lines we have thus far observed.

Since several of the assignments presented here rely on intensity measurements, some remarks about the quality and reliability of these measurements are clearly in order. In general, the observed intensities depend on the density of molecules produced in the jet, the FIR laser power, the microwave power, and the throughput of various optical elements, as well as on atmospheric absorptions—especially by H_2O. Relative intensity measurements made in the course of broad survey scans are thus not especially useful. The exception to this scenario is the case for lines observed within the same scan or in consecutive scans (within ~100 MHz of each other). For such lines, we are able to record accurate relative intensities, limited only by the S/N of the observed transitions. In establishing the assignments, we have primarily made use of the relative intensities of such closely spaced lines. For one subband ($A_3 \leftarrow A_1$) it was found necessary to make use of the relative intensities of lines spaced by 0.5–1.0 GHz. We have attempted somewhat more careful measurements of the laser power for these measurements, but they are, in any case, less reliable.

D. Energy level diagram

A qualitative ordering of the relative energies of the various tunneling states for the ground rotational state in the $(2C_3 + I)$ limit was presented by Nelson and Klemperer.[20] Although we have now measured spectra involving four new tunneling states not sampled by Nelson *et al.*[5,6] in their MBER studies, we can actually add little quantitative support for this proposed energy level scheme, because we have not yet observed any spectral features which contain a common level. We have measured spectra originating in both $K_a = 0$ and $K_a = 1$ levels of the ground state, and on the basis of these observations, we suggest that the energy level ordering of the tunneling states in $K_a = 1$ may actually be reversed from that in $K_a = 0$. The proposed picture is shown in Fig. 5, where we show both the ground and vibrationally excited levels, along with the vibration tunneling transitions

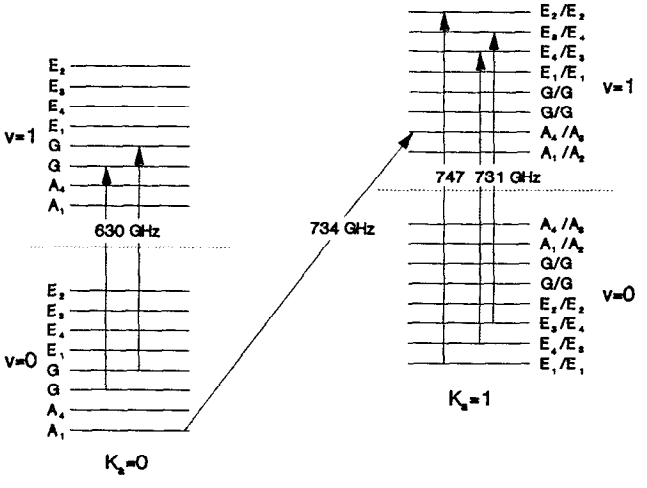

FIG. 5. Vibrational energy level diagram for $(NH_3)_2$.

which have been observed. This figure is drawn to be consistent with the following assumptions: (1) The observed intermolecular vibration is of A_2 symmetry; (2) the plane of symmetry is in the a–b molecular plane in both the ground and the excited state; (3) the interchange tunneling motion proceeds via a trans pathway.

As has now been well documented for monomers and dimers,[3] molecules relax by collisions according to dipole selection rules in supersonic jets. The rapid cooling that obtains thus preserves the equilibrium distribution among different VRT manifolds which are not connected by electric dipole transitions. For example, collisional transitions between A and E manifolds of the NH_3 monomer are forbidden. In a 5 K expansion,[27] we expect to have the temperature define only the relative population within each manifold, while the relative population in the different manifolds will be defined by the spin statistics associated with each symmetry.

The primary new experimental evidence pertaining to the ordering of the tunneling sublevels is the observation of three subbands assigned to the $K_a = 1$ E tunneling sublevels of the ground vibrational state, principally on the basis of their similar (unresolved) hyperfine envelopes. The measured intensities of these transitions, relative to those originating in the $K_a = 0$ G, states is approximately 6:1.

An exact calculation of the expected intensity ratios would require the knowledge of the energy separation between the different rotational and tunneling sublevels, and of $T_{\rm rot}$. Nevertheless, we can state that for the case of complete relaxation of all E sublevels into the $K_a = 1$ manifold, an intensity ratio of 4:1–8:1 is expected. If the E state ordering was not inverted, meaning that if the $K_a = 1$ E state was 130 GHz above the $K_a = 0$ E state, and therefore at least 130 GHz above the $K_a = 0$ G state, a ratio of 12:1 or more (G, $K_a = 0$:E, $K_a = 1$) would be expected.

Because of the above, and because we do not observe any transitions associated with the $K_a = 0$ E states, the energy level ordering and the large energy difference between $K_a = 1$ E sublevels and $K_a = 0$ sublevels shown in Fig. 5 appears to adequately explain the available data. Other explanations, including the scenario that we have simply not scanned in the correct frequency region for the $K_a = 0$ E transitions, are possible, however. The present energy level ordering was initially proposed by Hougen and Coudert,[34] it can be explained within the context of a high barrier analysis such as they employ in the study of $(H_2O)_2$. It remains to be seen whether or not such an analysis can be fruitfully employed for $(NH_3)_2$, especially in view of the extremely flat potential surface which is evidenced both in *ab initio* calculations and by the present observation of $a \sim 25$ cm^{-1} vibrational frequency.

IV. ANALYSIS

A. Rotational assignment

We have been able to assign six separate subbands to intermolecular vibration–rotation tunneling transitions, as listed in Table IV. The subbands sample levels of $K_a = 0$ and $K_a = 1$, and have been fit to a Watson S-reduced Hamiltonian:

$$E(K_a = 0) = \nu + \left(\frac{B+C}{2}\right) J(J+1) - D_J J^2 (J+1)^2 + H_J J^3 (J+1)^3$$

and

$$E^{\pm}(K_a = 1) = \nu + \left(\frac{B+C}{2}\right) J(J+1) - D_J J^2 (J+1)^2 + H_J J^3 (J+1)^3 \pm \left[\left(\frac{B-C}{4}\right) J(J+1) + d_1 J^2 (J^2+1) + h_1 J^3 (J+1)^3\right]. \quad (1)$$

The results of the fits are given in Table V where the constants labeled b.o. represent the band origins, and are equal to A plus ν, the intermolecular vibrational frequency, where appropriate. The signs of the constants $(B - C)$, d_1, and h_1, are consistent with the assumption that $(B - C)$ is negative for all vibrationally excited states. None of these subbands share a common level.

The two subbands in Table IV (A) and IV (B) are assigned as $K_a = 0 \leftarrow 0$ transitions. The two available $J = 2 \leftarrow 0$ combination differences indicate that the ground states of these two subbands are the same two G symmetry tunneling sublevels of the lower vibrational state observed in the microwave study of Nelson *et al.*[5,6] Using these combination differences, the bands were individually assigned as G_α and G_β. In the final fit, the hyperfine-corrected $R(0)$ and $R(1)$ pure rotational transitions from Nelson *et al.*[5] were included, with weights chosen according to the inverse of the square of their experimental uncertainties. A scan showing the R (1) line of the $G_\beta \leftarrow G_\beta$ subband is presented in Fig. 6.

The transitions in Table IV (C) are assigned as $A_3 \leftarrow A_1$, $K_a = 1 \leftarrow 0$. The R (4) line is shown in Fig. 7. The lines show a substructure, which is caused by a partially resolved hyperfine splitting. The observation of a Q branch indicates that the band is a perpendicular type band.

Three subbands are assigned to the E tunneling sublevels. Representative spectra for two of them are given in Fig. 8. The $E_2 \leftarrow E_1$ subband was assigned as a $K_a = 1 \leftarrow 1$ transition, based on the observation of a resolvable K type splitting (ranging from 1 to 40 MHz), the presence of $P(2)$ and $R(1)$ lines, and the absence of $R(0)$ and $P(1)$ lines. In contrast to the rather small K-type splitting in the $E_2 \leftarrow E_1$ subbands, the two $E_3 \leftrightarrow E_3$, $E_4 \leftrightarrow E_4$, $K_a = 1 \leftarrow 1$ series show a large K-type splitting (1 to 12 GHz). The band origins of these two subbands differ by only 38 MHz. This assignment of these two bands is based on the following facts: Neither $P(1)$ nor $R(0)$ could be found despite searches with more than adequate sensitivity. $R(1)$ is not observable due to atmospheric water absorption. Observation of the $Q(1)$ transition indicates that this must, therefore, be a $K_a = 1 \leftarrow 1$ subband. Alternative assignments of the data were tested in order to avoid the unusual result that the K-type splitting is large compared to the difference between the band origins. Assignment of the transitions spaced by 38 MHz as a K-type doublet within a single tunneling state, as well as the other possibilities gave unreasonable K-type splittings, or an un-

TABLE IV. VRT bands assigned in this work.

v'	J'	K_a'	K_c'	v''	J''	K_a''	K_c''	Obs.	Calc.	(Obs. − Calc.)	Weight
						(A) K_a: 0←0 $G_\alpha \leftarrow G_\alpha$					
1	10	0	10	0	9	0	9	717 503.6	717 503.6	0.0	0.0001
1	9	0	9	0	8	0	8	707 464.0	707 464.2	−0.2	0.0001
1	8	0	8	0	7	0	7	697 332.3	697 332.1	0.2	0.0001
1	7	0	7	0	6	0	6	687 117.9	687 117.6	0.3	0.0001
1	6	0	6	0	5	0	5	676 830.1	676 830.8	−0.7	0.0001
1	5	0	5	0	4	0	4	666 485.1	666 484.8	0.3	0.0001
1	4	0	4	0	3	0	3	656 097.9	656 097.5	0.4	0.0001
1	2	0	2	0	1	0	1	635 294.5	635 294.9	−0.4	0.0001
1	1	0	1	0	0	0	0	624 934.5	624 934.3	0.2	0.0001
1	0	0	0	0	1	0	1	604 415.0	604 414.8	0.2	0.0001
1	1	0	1	0	2	0	2	594 273.6	594 273.8	−0.2	0.0001
0	2	0	2	0	1	0	1	20 439.9552[a]	20 439.955 23	−0.000 03	1.0
0	1	0	1	0	0	0	0	10 220.6124[a]	10 220.612 37	0.000 03	1.0
	Standard deviation of the fit = 0.43 MHz										
						(B) K_a: 0←0 $G_\beta \leftarrow G_\beta$					
1	11	0	11	0	10	0	10	725 694.9	725 695.0	−0.1	0.0001
1	10	0	10	0	9	0	9	715 818.8	715 818.7	0.1	0.0001
1	9	0	9	0	8	0	8	705 850.9	705 850.6	0.3	0.0001
1	8	0	8	0	7	0	7	695 796.5	695 797.1	−0.6	0.0001
1	7	0	7	0	6	0	6	685 665.7	685 665.6	0.1	0.0001
1	6	0	6	0	5	0	5	675 466.0	675 466.0	0.0	0.0001
1	5	0	5	0	4	0	4	665 211.7	665 211.2	0.5	0.0001
1	4	0	4	0	3	0	3	654 916.9	654 917.0	−0.1	0.0001
1	3	0	3	0	2	0	2	644 601.9	644 601.7	0.2	0.0001
1	2	0	2	0	1	0	1	634 283.9	634 284.8	−0.9	0.0001
1	1	0	1	0	0	0	0	623 985.9	623 985.5	0.4	0.0001
1	0	0	0	0	1	0	1	603 499.4	603 499.2	0.2	0.0001
1	1	0	1	0	2	0	2	593 324.1	593 324.1	0.0	0.0001
0	2	0	2	0	1	0	1	20 440.5632[a]	20 440.5632	0.0000	1.0
0	1	0	1	0	0	0	0	10 220.9164[a]	10 220.9163	0.0001	1.0
	Standard deviation of the fit = 0.46 MHz										

(C) K_a: 1←0 $A_3 \leftarrow A_1$

v'	J'	K_a'	K_c'	v''	J''	K_a''	K_c''	Obs. Freq. (MHz)	o − c (MHz)
1	9	1	9	0	8	0	8	813 058.2	−0.2
1	7	1	7	0	6	0	6	795 704.2	−0.2
1	6	1	6	0	5	0	5	786 744.4	0.2
1	5	1	5	0	4	0	4	777 595.5	0.4
1	4	1	4	0	3	0	3	768 257.0	−0.2
1	3	1	3	0	2	0	2	758 731.3	0.5
1	1	1	1	0	0	0	0	739 115.0	0.3
1	1	1	0	0	1	0	1	728 791.4	−0.9
1	2	1	1	0	2	0	2	728 323.8	0.5
1	3	1	2	0	3	0	3	727 619.0	−1.4
1	4	1	3	0	4	0	4	726 683.4	−1.2
1	5	1	4	0	5	0	5	725 518.2	1.4
1	6	1	5	0	6	0	6	724 117.7	−1.0
1	7	1	6	0	7	0	7	722 491.9	0.1
1	8	1	7	0	8	0	8	720 637.2	−0.9
1	9	1	8	0	9	0	9	718 561.3	1.5
1	10	1	9	0	10	0	10	716 260.5	1.0
1	11	1	10	0	11	0	11	713 739.1	−1.0
1	1	1	1	0	2	0	2	708 299.0	1.5
1	2	1	2	0	3	0	3	697 659.2	0.2
1	3	1	3	0	4	0	4	686 840.1	−0.2
1	4	1	4	0	5	0	5	675 842.8	−0.4
1	5	1	5	0	6	0	6	664 669.9	−0.4
1	6	1	6	0	7	0	7	653 323.6	−0.2
1	7	1	7	0	8	0	8	641 806.7	0.1
1	8	1	8	0	9	0	9	630 121.7	0.4
	Standard deviation of the fit = 0.9 MHz								
						(D) K_a: 1←1 $E_{2/1} \leftarrow E_{1/2}$			
1	8	1	8	0	7	1	7	823 801.2	0.6
1	8	1	7	0	7	1	6	823 779.3	0.6
1	7	1	7	0	6	1	6	814 723.2	−0.8
1	7	1	6	0	6	1	5	814 706.6	−0.8

TABLE IV. (*continued*).

v'	J'	K_a'	K_c'	v''	J''	K_a''	K_c''	Obs. Freq. (MHz)	o − c (MHz)
				(D) K_a: $1 \leftarrow 1$ $E_{2/1} \leftarrow E_{1/2}$					
1	5	1	5	0	4	1	4	796 145.8	− 0.9
1	5	1	4	0	4	1	3	796 137.7	− 0.9
1	4	1	4	0	3	1	3	786 643.2	0.9
1	4	1	3	0	3	1	2	786 638.2	0.9
1	3	1	3	0	2	1	2	776 993.4	1.1
1	3	1	2	0	2	1	1	776 990.8	1.2
1	2	1	2	0	1	1	1	767 195.4	− 0.6
1	2	1	1	0	1	1	0	767 194.4	− 0.6
1	1	1	1	0	2	1	2	726 551.8	− 0.9
1	1	1	0	0	2	1	1	726 549.8	− 1.0
1	2	1	2	0	3	1	3	716 033.1	0.5
1	2	1	1	0	3	1	2	716 028.9	0.4
1	3	1	3	0	4	1	4	705 372.7	0.1
1	3	1	2	0	4	1	3	705 365.7	0.0
1	4	1	4	0	5	1	5	694 576.0	0.5
1	4	1	3	0	5	1	4	694 565.4	0.4
1	5	1	5	0	6	1	6	683 644.1	− 0.4
1	5	1	4	0	6	1	5	683 629.5	− 0.2
1	6	1	6	0	7	1	7	672 583.4	− 0.0
1	6	1	5	0	7	1	6	672 563.8	0.2
1	7	1	7	0	8	1	8	661 396.4	− 0.1
1	7	1	6	0	8	1	7	661 370.4	− 0.5
1	9	1	9	0	10	1	10	638 665.1	0.5
1	9	1	8	0	10	1	9	638 625.6	0.5
1	10	1	10	0	11	1	11	627 130.2	− 0.3
1	10	1	9	0	11	1	10	627 082.8	− 0.2
	Standard deviation of the fit = 0.74 MHz								
				(E) K_a: $1 \leftarrow 1$ $E_{3/4} \leftarrow E_{3/4}$					
1	11	1	10	0	10	1	9	809 226.7	
1	10	1	10	0	9	1	9	819 077.4	0.2
1	9	1	9	0	8	1	8	811 260.7	− 0.2
1	9	1	8	0	8	1	7	799 175.1	0.1
1	7	1	7	0	6	1	6	794 983.7	− 0.6
1	7	1	6	0	6	1	5	787 522.9	− 2.1
1	6	1	6	0	5	1	5	786 515.4	1.3
1	6	1	5	0	5	1	4	781 034.4	2.3
1	5	1	5	0	4	1	4	777 817.2	0.8
1	5	1	4	0	4	1	3	774 064.9	1.9
1	4	1	4	0	3	1	3	768 887.0	− 0.8
1	4	1	3	0	3	1	2	766 578.8	− 1.6
1	3	1	3	0	2	1	2	759 725.7	0.1
1	3	1	2	0	2	1	1	758 542.7	− 2.2
1	1	1	0	0	1	1	1	730 577.4	0.7
1	1	1	1	0	1	1	0	730 200.7	− 1.8
1	1	1	1	0	2	1	2	710 372.6	2.0
1	1	1	0	0	2	1	1	709 228.0	− 0.7
1	2	1	2	0	3	1	3	699 798.0	2.1
1	2	1	1	0	3	1	2	697 539.7	− 1.3
1	3	1	3	0	4	1	4	688 991.2	0.0
1	3	1	2	0	4	1	3	685 303.7	1.3
1	4	1	4	0	5	1	5	677 956.0	− 2.7
1	4	1	3	0	5	1	4	672 552.3	0.9
1	5	1	5	0	6	1	6	666 697.8	− 2.3
1	5	1	4	0	6	1	5	659 321.0	− 1.0
1	6	1	6	0	7	1	7	655 218.9	2.7
1	8	1	8	0	9	1	9	631 568.3	− 0.1
	Standard deviation of the fit = 2.0 MHz								
				(F) K_a: $1 \leftarrow 1$ $E_{4/3} \leftarrow E_{4/3}$					
1	11	1	10	0	10	1	9	809 203.8	
1	10	1	10	0	9	1	9	819 019.7	− 0.6
1	9	1	9	0	8	1	8	811 209.5	0.9
1	9	1	8	0	8	1	7	799 148.4	1.3
1	8	1	7	0	7	1	6	793 530.9	− 4.4
1	7	1	7	0	6	1	6	794 940.1	− 0.6
1	7	1	6	0	6	1	5	787 492.9	2.4
1	6	1	6	0	5	1	5	786 473.4	0.6
1	6	1	5	0	5	1	4	781 002.5	3.6

TABLE IV. (*continued*)

(F) K_a: $1 \leftarrow 1$ $E_{4/3} \leftarrow E_{4/3}$

v'	J'	K_a'	K_c'	v''	J''	K_a''	K_c''	Obs. Freq. (MHz)	o − c (MHz)
1	5	1	5	0	4	1	4	777 776.8	0.1
1	5	1	4	0	4	1	3	774 030.8	0.4
1	4	1	4	0	3	1	3	768 848.5	−0.1
1	4	1	3	0	3	1	2	766 543.6	−3.1
1	3	1	3	0	2	1	2	759 687.1	0.9
1	3	1	2	0	2	1	1	758 506.0	−3.1
1	1	1	0	0	1	1	1	730 539.2	1.9
1	1	1	1	0	1	1	0	730 163.1	−1.0
1	1	1	1	0	2	1	2	710 333.9	2.6
1	1	1	0	0	2	1	1	709 190.7	−1.8
1	2	1	2	0	3	1	3	699 758.4	2.0
1	2	1	1	0	3	1	2	697 506.1	−0.8
1	3	1	3	0	4	1	4	688 950.8	−0.1
1	3	1	2	0	4	1	3	685 269.8	0.0
1	4	1	4	0	5	1	5	677 913.6	−3.0
1	4	1	3	0	5	1	4	672 520.0	1.0
1	5	1	5	0	6	1	6	666 652.9	−2.4
1	5	1	4	0	6	1	5	659 290.4	−0.3
1	6	1	6	0	7	1	7	655 171.4	3.2
1	8	1	8	0	9	1	9	631 515.5	−0.7

Standard deviation of the fit = 2.5 MHz

[a] From Ref. 3.

TABLE V. Obtained constants for all assigned $(NH_3)_2$ subbands in MHZ. (b.o.) is the band origin of the corresponding subband.

(A)	Lower State	(a) $G_aK_a = 0$	(b) $G_\beta K_a = 0$	(c) $A_1K_a = 0$
	$(B'' + C'')/2$	5110.528 2(75)	5110.608 5(67)	5136.517 (97)
	$(B'' - C'')$			
	D_J''	0.134 5(17)	0.086 7(10)	0.039 49(42)
	d_1''			
	H_J''	0.011 73(21)	0.005 75(12)	
	H_1''			
	Excited State	$G_aK_a = 0$	$G_\beta K_a = 0$	$A_3K_a = 1$
	$(B' + C')/2$	5 150.93(18)	5 133.60(13)	5 031.604(54)
	$(B' - C')$			−49.625(54)
	D_J'	0.750 3(60)	0.461 9(39)	0.047 70(39)
	d_1'			0.001 42(17)
	H_J'	0.009 71(15)	0.004 925(91)	
	b.o.	614 635.41(30)	613 720.15(30)	734 058.62(39)

(B)	Lower State	(d) $E_{1/2}K_a = 1$	(e) $E_{3/4}K_a = 1$	(f) $E_{4/3}K_a = 1$
	$(B'' + C'')/2$	5 117.256(38)	5 150.10(36)	5 149.70(41)
	$(B'' - C'')$	0.607(38)	384.39(36)	383.25(41)
	D_J''	0.054 28(27)	0.333 4(61)	0.317 8(54)
	d_1''		−0.274 1(39)	−0.266 9(43)
	H_J''		0.001 355(58)	0.001 200(51)
	H_1''		0.001 085(40)	0.000 990(41)
	Excited State	$E_{2/1}K_a = 1$	$E_{3/4}K_a = 1$	$E_{4/3}K_a = 1$
	$(B' + C')/2$	5 044.396(47)	4 933.97(25)	4 933.98(32)
	$(B' - C')$	−0.136(47)	−8.03(25)	−7.88(32)
	D_J'	0.033 85(41)	0.031 2(24)	0.030 4(25)
	d_1'		0.005 0(16)	0.003 8(20)
	H_J'		0.000 200(20)	0.000 182(19)
	b.o.	747 091.80(28)	730 604.5(1.7)	730 565.3(1.4)

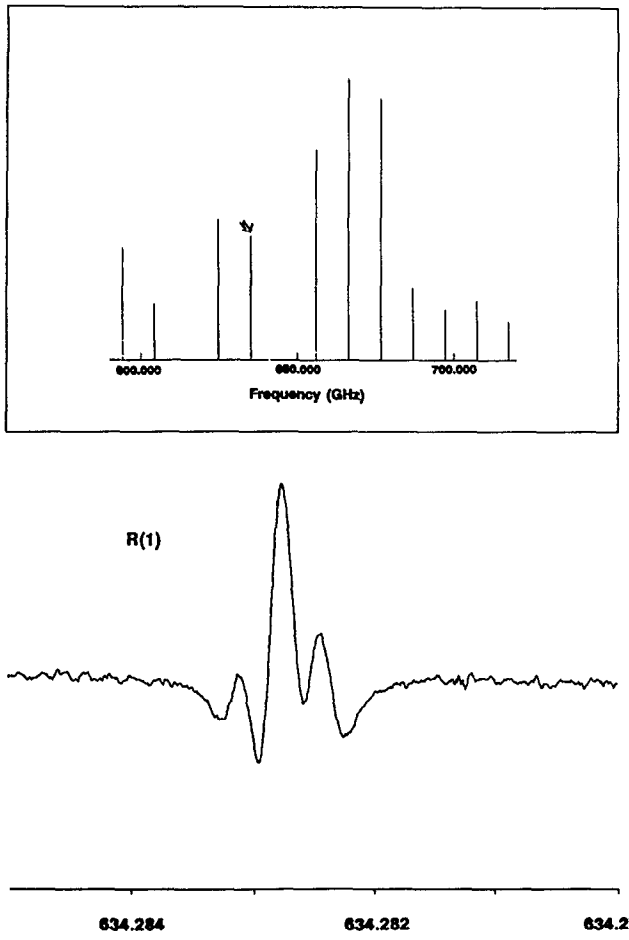

FIG. 6. Stick spectrum of $G_\beta \leftarrow G_\beta$ subband together with a typical line.

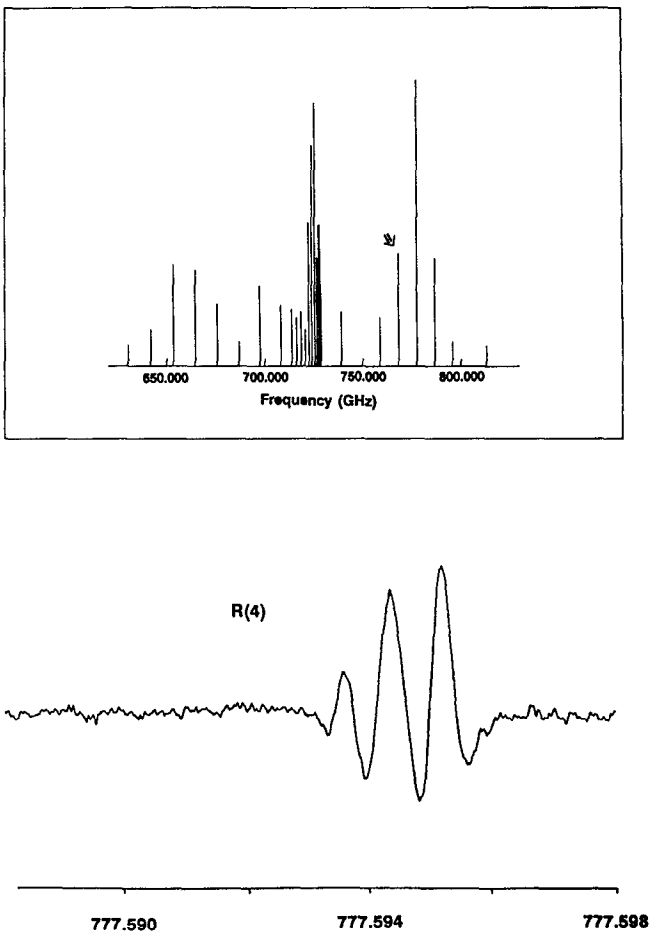

FIG. 7. Stick spectrum of $K_a = 0\ A_3 \leftarrow A_1$ with a typical line.

reasonable increase in the standard deviation of the fit. Although we believe that the $R(10)$ transitions listed in Table IV E and IV F belong to these two E-type subbands because they have the proper splittings and line shapes resulting from unresolved hyperfine, these lines were not included in the fit because doing so results in a factor of 2 increase in the standard deviation of the fit. The lower states of the $E_{3/4}$ subbands appear to be perturbed. In particular, we note the unphysically large asymmetry parameter required to fit the data. Also, the standard deviation of the fit is 2.6 MHz, which is more than twice the experimental uncertainty, whereas the other bands are fit considerably better.

For ordinary semirigid molecules, the determination of the asymmetry parameters for seven different vibration tunneling states would allow some deductions to be made regarding structure of the molecule. However, in the present case, the apparent perturbation in the E_3 and E_4 tunneling sublevels of the ground state, and the large variation in $B - C$ among the other states serves only as evidence that the molecule is extremely fluxional. We find that $(B - C)$ in the upper states of the $K_a = 1 \leftarrow 1$ subbands changes sign relative to the lower states. If $(B - C)$ is, in fact, negative for all vibrationally excited states and positive for all tunneling states sampled in the ground vibrational state, then this unusual result could be related to the symmetry of the intermolecular vibration. It is possible that the two axes switch in the vibrationally excited state (i.e., the b axis of the ground state becomes the c axis of the vibrationally excited level, both corresponding to the x axis of the molecule-fixed frame). Such an axis switching would interchange the relative energies of the two symmetry species of the K-type doublets for $K_a =$ odd, while having no observable consequences for states with $K_a =$ even. Unfortunately, other reasonable explanations exist for the observed sign alternation in $(B - C)$, including the possibility of an A_2 vibration, and hence no definitive conclusions can be drawn at this stage.

B. Tunneling assignment

The tunneling assignment of the two G subbands was straightforward because of the available combination differences. According to the selection rules, the two observed G bands must be pure vibrational transitions ($G_\alpha \leftarrow G_\alpha$, $G_\beta \leftarrow G_\beta$), or they both could be vibration tunneling transitions, ($G_\beta \leftarrow G_\alpha$, $G_\alpha \leftarrow G_\beta$.) Possibilities involving one tunneling and one nontunneling transition require a common upper state, and thus are easily eliminated since this was not found to be the case. Reasonable estimates place the interchange tunneling splitting at a few tens of GHz. This follows from analogy to both $(H_2O)_2$ and $(HF)_2$, for which the interchange frequencies are 19.0 (Ref. 3) and 19.8 (Ref. 1) GHz, respectively, and from the fact that no tunneling tran-

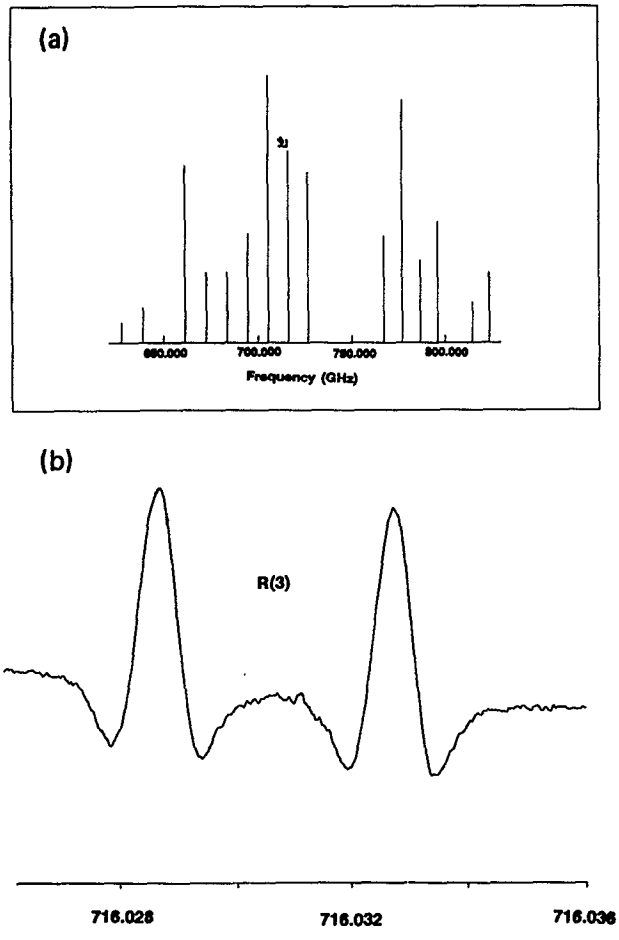

FIG. 8. (a) Stick spectrum and typical line for the $E_2 \leftarrow E_1$, $K_a = 1 \leftarrow 1$. (b) Stick spectrum and typical line for the $E_{3/4} \leftarrow E_{3/4}$ subband.

sitions were observed in the microwave experiments of Nelson *et al.*[5,6] The pair of vibration tunneling subbands would be expected to be separated roughly by the sum of the interchange frequencies in the ground and vibrationally excited states. Since the two observed G subbands are separated by a much smaller frequency (1 GHz), we assign them as nontunneling transitions: $G_\alpha \leftarrow G_\alpha$ and $G_\beta \leftarrow G_\beta$

As can be seen in Fig. 8(a), the two components of the K-type doublets belonging to lines in the $K_a = 1 \leftarrow 1$ subband whose origin is 747 GHz have identical intensity. Only four tunneling sublevels can have K-type doublets with a 1:1 intensity ratio. These are the two G, the E_1, and the E_2 tunneling states. Since we do not observe a second nearby state, this transition must be a tunneling $G_\beta \leftarrow G_\alpha$, $G_\alpha \leftarrow G_\beta$ pair if it involves the G states. However, if tunneling transitions G_α and G_β are allowed, both G states should be in thermal equilibrium at $T_{\rm rot}$. If no such dipole transitions are possible, the population distribution among those levels is governed by $T_{\rm tun}$, which is considerably higher than $T_{\rm rot}$, as discussed before. Despite the extremely low jet temperature ($T_{\rm rot} = 1$ K) reported by Nelson *et al.*[6] their observed intensity ratio between identical rotational lines of different G states excludes the possibility of relaxation processes among those tunneling states. This implies that tunneling $G_\alpha \leftarrow G_\beta$, $G_\alpha \leftarrow G_\beta$, transitions are forbidden. We therefore assign the observed transition as either $E_2 \leftarrow E_1$ or $E_1 \leftarrow E_2$. We are presently unable to distinguish between these two possibilities. For simplicity, we will refer to this subband as $E_2 \leftarrow E_1$ in what follows.

The two $K_a = 1 \leftarrow 1$ parallel subbands whose origins are at 731.565 and 731.603 GHz are assigned as $E_3 \leftarrow E_3$ and $E_4 \leftarrow E_4$. The small spacing between the band origins is indicative of a pair of transitions occurring with no change in tunneling state. In the $(2C_3 + I)$ limit, only two such transitions are permitted, viz. among the two G states, or $E_3 \leftarrow E_3$ and $E_4 \leftarrow E_4$. For both the subband assigned above as $E_2 \leftarrow E_1$ and for this pair assigned $E_3 \leftarrow E_3$, $E_4 \leftarrow E_4$, we are forced to choose between assignment to sublevels of E symmetry or of G symmetry. The unresolved hyperfine envelopes and their J dependences are similar in these three subbands; we therefore can logically assign all three transitions as either $E \leftarrow E$ or $G \leftarrow G$. Since there are six unique sublevels involved (i.e., having no common levels), whereas only two $K_a = 1$ vibration tunneling G states occur for each vibrational level, we assign these transitions as occurring among the E states. The assignment is based upon the assumption that it is more likely that all E states will exhibit the same hyperfine structure than the possibility that G and E states will show the same hyperfine structure pattern, especially since the interchange tunneling should be quenched in the G states. Furthermore, careful measurements were performed to compare the intensities of identical rotational transitions in the $E_3 \leftarrow E_3$ and $E_4 \leftarrow E_4$ subband. This indicated that identical rotational transitions from both tunneling subbands have the same spin statistical weight. By inspecting Fig. 2, we find that this requires the assumption of an interaction which switches the ordering of one of the K-type doublets (as shown in Fig. 4). We note that the above considerations could also permit assignment of the nontunneling transitions to the $K_a = 1$ G states, which we assume to have a different hyperfine structure.

Finally, we turn to the perpendicular $K_a = 1 \leftarrow 0$ transition. Measurement of the relative intensities of several Q branch lines indicates a ratio of $J_{\rm odd}/J_{\rm even}$ of 1.25(15). This indicates that the lower state is either A_1 or E_4, for which the theoretical relative intensities of $J_{\rm odd}/J_{\rm even}$ are ~78/66 (1.18) and 42/30 (1.43), respectively. The other bands with such intensity alternation originate in the A_4 and E_3 sublevels, but have expected relative intensities of $J_{\rm odd}/J_{\rm even}$ of 66/78 (0.85); 30/42 (0.71), which are inconsistent with the observed ratio. Since we expect that the $K_a = 0$ E levels are significantly depleted by collisional relaxation into the $K_a = 1$ E levels, and a comparison with the combination differences of the already assigned vibrationally excited $K_a = 1$ E_4 state showed no coincidences, we assign this transition as $A_3 \leftarrow A_1$. It should also be noted that the rotational constants of this subband are close to the structural values.

C. Hyperfine structure

Nelson *et al.*[5,6] were able to use the ^{14}N quadrupole hyperfine structure from a number of different isotopes to obtain structural information about $(NH_3)_2$. In particular, the angle between the C_3 axis of an NH_3 monomer and the *a*

axis of the cluster is given by the relation

$$eqQ_{aa} = \frac{eqQ_{NH_3}}{2}(3\cos^2\theta - 1), \quad (2)$$

where eQq_{aa} is the measured nuclear quadrupole coupling constant of the complex, eqQ_{NH_3} is the nuclear quadrupole coupling constant for a NH_3 monomer, and θ is the relevant angle.

Unfortunately, the nitrogen quadrupole coupling constants are too small to allow for an accurate determination of the hyperfine constants in all of the states we have measured, given the resolution of the FIR laser experiment. For the G states, we were able to fix the ground state hyperfine constants at the values obtained by Nelson *et al.* and thus determine the upper state hyperfine constants. The constants thus determined are explicitly for the G_β state, although one does not expect significantly different results for the G_α state. A combined weighted fit of the assigned hyperfine components for the $R(2)$, $R(1)$, and $P(2)$ transitions in the G_β state, including lines from Nelson *et al.*,[5] was used to obtain an estimate for the hyperfine parameter in the vibrationally excited state. The calculations were carried out using Pickett's general vibration–rotation program.[35] The fit yielded the following results for the excited state:

$$eqQ^1_{aa} = 1.80(18)\ \text{MHz}$$

$$eqQ^2_{aa} = -0.50(25)\ \text{MHz}.$$

These parameters resulted in the following constraints on the excited state angles θ_1 and θ_2, assuming that the structure in these G states are sufficiently rigid to justify their extraction from the expectation value of P_2:

$$94 < \theta_1 < 105,\ 48 < \theta_2 < 52.$$

These are then compared with the angles determined for the lower state:[2]

$$\theta_1 = 115.5(1)\ \ \theta_2 = 48.6(1).$$

Detailed analysis of the hyperfine structure of the other states was impeded by inadequate resolution, and by the requirement for four independent parameters to describe the hyperfine structure in $K_a = 1$ sublevels. However, we investigated the qualitative features of the observed hyperfine structure for three different cases: (1) The hyperfine constants of all states were held fixed at the ground state values for the $K_a = 0$ G states. (2) The observed hyperfine structure was assumed to result from averaging over the tunneling motion, assuming a *trans* interchange tunneling path. The expectation value of $P_2(\cos\theta)$ for this path produces $eqQ_{aa} = 0.181$ MHz. The value of eqQ_{aa} is, in this case, identical for both nuclei, due to the rapid interchange tunneling. (3) The hyperfine structure was taken to be the average value resulting from the *cis* tunneling path, giving $eqQ_{aa} = -3.972$ MHz. The additional parameter $(eqQ_{bb} - eqQ_{cc})$ was taken from the relation[26]

$$(eqQ_{aa} + eqQ_{bb} - eqQ_{cc}) = eqQ_{NH_3}, \quad (3)$$

which is valid if complex formation does not substantially affect the field gradients at the nuclei. The pattern obtained when employing the *cis* path averaged parameters predicted a hyperfine structure spread over several MHz, in contrast to our measurements, which evidence a much more confined splitting. Neither of the other models used actually reproduce the observed data either, but the differences were much less striking.

The hyperfine measurements thus argue against a *cis* tunneling path for the exchange tunneling. However, only an improved determination of the hyperfine structure in the various tunneling states will allow us to obtain a more detailed understanding of the nature of the actual tunneling path.

D. Vibrational assignment

There are six intermolecular vibrational modes in $(NH_3)_2$. Several *ab initio* calculations have predicted the existence of a very low lying vibrational frequency in $(NH_3)_2$, although none of these same calculations actually reproduce the experimental geometry. Both Dykstra and co-workers[17,19] and Frisch and co-workers[36] calculate a harmonic frequency of $\sim 25\ \text{cm}^{-1}$ for the lowest intermolecular vibration (a torsion). Our observation of the two nontunneling G state transitions, as well as the transitions connecting $E_3 \leftarrow E_3$ and $E_4 \leftarrow E_4$, establish the existence of a vibrational state of the complex $\sim 25\ \text{cm}^{-1}$ above the ground state. We note that the above *ab initio* calculations give A'' as the symmetry (in the C_s limit) of the lowest excited vibrational state.

The available information is not sufficient to determine the symmetry of the vibration in G_{36}. Because of the ambiguity in the symmetry label of the vibrational wave function, we cannot determine if the transitions originating in the A_1 and E_1 sublevels are actually tunneling or nontunneling in nature. The selection rules for the other four transitions forbid tunneling in the $(2C_3 + I)$ limit regardless of vibrational symmetry.

We are also presently limited in our ability to characterize the nature of the vibrational motion because of the extreme variations observed in the rotational constants. The hyperfine constants for the two $K_a = 0 \leftarrow 0$ G subbands provide the most clear indication at this point. The measured values of the quadrupole coupling constant indicate a decrease in θ_1 from 115.5(1)° in the ground state to 99.5(5.5) in the upper state, and an increase in θ_2 from 48.6(1)° in the ground state to 50(2)° in the upper state. This constitutes some evidence for torsional motion. The relatively large angular change that apparently occurs upon vibrational excitation should significantly affect the facility with which the two NH_3 subunits interchange roles. Establishing the interchange frequencies in the ground and excited states would thus be particularly interesting.

V. DISCUSSION

In the preceding sections, we have detailed the assignment of six FIR-subbands to tunneling subbands of a low frequency intermolecular vibration. These assignments are made on the basis of detailed group theoretical arguments, extending the work of Nelson and Klemperer.[20] This treatment has been carried out without the aid of a model poten-

tial, and relies on several assumptions: (1) G_{36} is the appropriate molecular symmetry group. (2) The existence of a plane of symmetry in the equilibrium structure of the complex. (3) The C_3 tunneling motion dominates the interchange tunneling ($2C_3 + I$ limit is appropriate). (4) Vibration tunneling and rotational motions of the complex are separable. (5) Interchange tunneling of inequivalent monomers occurs via a tunneling path of trans symmetry. Arguments presented in the preceding sections seem to justify these assumptions; at least the available data are consistent with them, and they correspond to established features of the much more thoroughly characterized $(HF)_2$ and $(H_2O)_2$ systems. Some experimental support for these assumptions is summarized below.

Our data support the assumption that G_{36} is the group which includes all feasible permutation inversion operations for $(NH_3)_2$. Groups smaller than G_{36}, such as G_{18} (including only internal rotation for each NH_3 monomer) or G_4 (including only the interchange motion), either would show no intensity alternations, as was found for the $A_3 \leftarrow A_1$ transition, or the selection rules would forbid pure rotational transitions, such as the $G \leftarrow G$ transitions observed by Nelson *et al.* If we would increase the group size to allow for motions which change the handedness of each NH_3 monomer (the umbrella inversion), then G_{144} becomes the molecular symmetry group. In this group, each rotational level would split into 22 levels, with 14 of them having nonzero spin statistical weight; twelve of these would be G states, and there would be one A and one B state. Therefore, we would expect to see several G state transitions, and particularly, we should observe more than two nontunneling transitions. This was clearly not the case; moreover, measurements of other NH_3 complexes[4] have shown, that in all complexes studied, except Ar–NH_3, the umbrella inversion is quenched by the anistropy of the intermolecular potential. In general, we were able to obtain a consistent description of all measured transitions within the group G_{36}.

In all the group theoretical considerations it was assumed that the ammonia dimer possesses a plane of symmetry. If the equilibrium structure cannot be described by C_s, there will be a further doubling of each of the states described by G_{36}. In addition to the tunneling motions mentioned before, a tunneling motion through the plane of symmetry will occur. Therefore, one would expect to observe *four* pure rotational transitions, due to the four populated G levels. Only if the different G states were separated by a large energy gap, such that collisional relaxion results in a considerable decrease in the population of the upper G states, will this assumption be in agreement with the observation of only *two* G levels by Nelson *et al.*.

The $(2C_3 + I)$ limit was proposed by Nelson *et al.* It is also consistent with the observation made here that the band origins of the two G subbands were found to be within 1 GHz of one another, whereas other parallel subbands (of E symmetry) are 130 GHz away. In addition, the rotational constants of both G states are quite similar, but these differ considerably from the constants found in the $K_a = 0$, A state. This can be explained in terms of the $(2C_3 + I)$ limit, wherein the two G levels are close in energy, but separated by a large energy difference from the A states.

The assumption of separability of rotation and tunneling motions is supported by the observation of only half of the transitions that would be allowed if they were, in fact, strongly coupled.

An overall energy level diagram which shows the transitions observed and assigned in this work is given in Fig. 5. It is based on the assumption of an intermolecular vibration of A_2 symmetry, a *trans* interchange tunneling pathway, and a plane of symmetry containing the a and b principal axes. The level sequence of the lower state is chosen as suggested by Hougen and Coudert.[34] The observed transitions put restrictions on the energy level sequence of the vibrationally excited state. In particular, our assignment of the $E_3 - E_4$ subbands for $K = 1$, forces us to assume a different energy level order for the vibrationally excited $K_a = 1$ state relative to the $K_a = 1$ ground state. No information on the level sequence in the $K_a = 0$ excited vibrational state is obtained, because only G states are accessed by our data.

The ordering of the K-type doublet components of the E_3 or E_4 tunneling states is switched, as discussed in Sec. IV B. This is accompanied by a large K-type splitting. Both effects require the assumption of an interaction which influences the $K_a = 1$ energy levels. A possible source would be the Coriolis interaction between the E_3, $E_4 K_a = 1$ levels. As can be seen in Fig. 5, the $K_a = 0$ E_3 and E_4 levels are separated by a tunneling splitting, whereas for $K_a = 1$ each tunneling state consists of a E_3 and E_4 symmetry species. In this picture, the Coriolis interaction, which causes interacting levels to repel, could lead to a switching of the K-type doublet components in one of the tunneling states (as shown in Fig. 5). The same switch would have to be assumed for the vibrationally excited state. The small energy difference between the two subbands (38 MHz), and the nearly identical parameters obtained for them, may indicate a small energy separation between the two tunneling energy levels.

A substantial variation of the effective rotational constants with the various tunneling and K_a states was found. Particularly, $(B - C)$ varies by a large amount (factor of 500 in the lower vibrational state), and only for the $A_3 \leftarrow A_1$ subband is it close to the structural parameter (70 MHz). The state with A_1 symmetry correlates to a noninternally rotating tunneling state. The values obtained for $(B - C)$ in the E and G states must therefore be attributed to perturbations by Coriolis interactions [as was found for $(H_2O)_2$][33] or to the J dependence of the tunneling splitting. The difference in the tunneling splittings between lower state and excited state will contribute both the effective rotational constant $(B + C)/2$ and to the effective asymmetry parameter $(B - C)/4$. The Coriolis interaction in $(H_2O)_2$ resulted in an asymmetry parameter which was 10 times larger than the structural value.[33]

As we can see from Table V, for all subbands other than the perturbed $K_a = 0$, $G \leftarrow G$ transition, the rotational constant B is smaller in the excited state than in the lower state. This corresponds to an increase in the average distance between the two NH_3 monomers, or to a stretching vibration. Associated with the stretch is an increase of the angle between the NH_3 monomer C_3 axis and the a axis of the dimer.

We do not get reliable values for the bond length changes involved, because, as pointed out before, the rotational constants do not reliably reflect the structural values. In general, B for the lower state varies by 0.8%, comparing the different K levels ($K_a = 1$ and $K_a = 0$) and tunneling states. A calculation of R_{CM}, the average distance between the centers of mass of the two NH_3 monomers, based on the rotational constant B will therefore not be more accurate than 0.4%. For the upper state, the calculated R_{CM} value changes by up to 2%. We should note that the spread of B values found for different tunneling states is considerably larger than found for $(H_2O)_2$.[3,33]

All observed G states seem to be perturbed. In contrast with the A_1 and A_3 states, distortion constants as high as H were necessary in order to fit the data. The $K_a = 0$ and $K_a = 1$ G states can interact with each other through a Coriolis interaction. This would change the effective rotational constants, $(B + C/2) = \overline{B}$, values of the two states in such a way that the $\overline{B}$ value of the lower state will be decreased, while the $\overline{B}$ value for the upper state will increase. The evidence for perturbation in the lower $K = 0$ G states is of particular significance, given the existing controversy over the equilibrium structure of the ammonia dimer. The structural determination of Nelson *et al.* is deduced exclusively from microwave measurements on these G states, and is based on the assumption that these states are nontunneling, and unperturbed, corresponding to a rigid molecular structure. In addition to the decrease in the effective rotational constant that results from the $K_a = 0 - K_a = 1$ mixing, the expectation values of $P_1(\cos\theta)$ and $P_2(\cos\theta)$ could also be perturbed. Since these properties, deduced from Stark effect and hyperfine measurements on the G states, were inverted to provide the angular characterization of the complex structure, error in the latter could also result from such a perturbation. These effects are probably relatively small, however, since the structure deduced by Nelson *et al.* did not vary significantly among different isotopomers, as it would be expected to if either Coriolis perturbations or zero-point effects were important.

ACKNOWLEDGMENTS

This work was supported by the Director, Office of Energy Research, Office of Basic Energy Sciences, Chemical Sciences Division of the U.S. Department of Energy under Contract No. DE-AC03-76SF00098. The FIR laser system was funded by the National Science Foundation Grant No. CHE-8612296. One of us (M.H.) wants to thank the Studienstiftung des Deutschen Volkes for financial support. We thank Dr. J. T. Hougen, Dr. L. H. Coudert, Professor W. Klemperer, and J. Loeser for their important contributions to this work. We would also like to thank Dr. H. M. Pickett for providing us with the general multispin, vibration–rotation fitting program CALFIT, which is available through the NASA COSMIC program.

[1] A. S. Pine and W. J. Lafferty, J. Chem. Phys. **78**, 2154 (1983); B. J. Howard, T. R. Dyke, and W. Klemperer, *ibid.* **81**, 5417 (1984); J. T. Hougen and N. Ohashi, J. Mol. Spectrosc. **109**, 134 (1985); H. S. Gutowsky, C. Chuang, J. D. Keen, T. D. Klots, and T. Emilsson, J. Chem. Phys. **83**, 2070 (1985); A. S. Pine, W. J. Lafferty, and B. J. Howard, *ibid.* **81**, 2939 (1984); Z. S. Huang, K. W. Jucks, and R. E. Miller, *ibid.* **85**, 3338 (1986); W. J. Lafferty, R. D. Suenram, and F. J. Lovas, J. Mol. Spectrosc. **123**, 434 (1987).

[2] N. Ohashi and A. S. Pine, J. Chem. Phys. **81**, 73 (1984); G. A. Blake, K. L. Busarow, R. C. Cohen, K. B. Laughlin, Y. T. Lee, and R. J. Saykally, *ibid.* **89**, 6577 (1988); N Moazzen-Ahmadi, A. R. W. McKellar, and J. W. C. Johns, J. Mol. Spectrosc. **138**, 282 (1989); G. A. Blake and R. E. Bumgarner, J. Chem. Phys. **91**, 7300 (1989); M. D. Schuder, C. M. Lovejoy, D. D. Nelson, Jr., and D. J. Nesbitt, *ibid.* **91**, 4418 (1989).

[3] L. H. Coudert, F. J. Lovas, R. D. Suenram, and J. T. Hougen, J. Chem. Phys. **87**, 6290 (1987); J. A. Odutola, T. A. Hu, D. Prinslow, S. E. O'dell, and T. R. Dyke, *ibid.* **88**, 5352 (1988); K. L. Busarow, R. C. Cohen, G. A. Blake, K. B. Laughlin, Y. T. Lee, and R. J. Saykally, *ibid.* **90**, 3937 (1989); G. T. Fraser, R. D. Suenram, and L. H. Coudert, *ibid.* **90**, 6077 (1989); Z. S. Huang and R. E. Miller, *ibid.* **91**, 6613 (1989).

[4] G. T. Fraser, D. D. Nelson, Jr., A. Charo, and W. Klemperer, J. Chem. Phys. **82**, 2535 (1985).

[5] D. D. Nelson, Jr., G. T. Fraser, and W. Klemperer, J. Chem. Phys. **83**, 6201 (1985).

[6] D. D. Nelson, Jr., W. Klemperer, G. T. Fraser, F. J. Lovas, and R. D. Suenram, J. Chem. Phys. **87**, 6364 (1987).

[7] K. Sagarik, R. Ahlrichs, and S. Brode, Mol. Phys. **57**, 1247 (1986).

[8] W. L. Jorgensen and M. Ibrahim, J. Am. Chem. Soc. **102**, 3309 (1980).

[9] Z. Latajka and S. Scheiner, J. Chem. Phys. **81**, 407 (1984).

[10] N. C. Baird, Int. J. Quant. Chem. **1**, 49 (1974).

[11] W. A. Sokalaki, P. C. Harlharan, and J. J. Kaufman, J. Phys. Chem. **87**, 2803 (1983).

[12] N. K. Ray, M. Shibatta, G. Bolis, and R. Rein, Int. J. Quant. Chem. **27**, 427 (1985).

[13] K. Ohta, Y. Toshioka, K. Morokuma, and K. Kitaura, Chem. Phys. Lett. **101**, 12 (1983).

[14] W. C. Topp and L. C. Allen, J. Am. Chem. Soc. **96**, 5291 (1974).

[15] H. Umeyama and K. Morokuma, J. Am. Chem. Soc. **99**, 1316 (1977).

[16] A. Hinchliffe, D. G. Bounds, M. L. Klein, I. R. McDonald, and R. Righini, J. Chem. Phys. **74**, 1211 (1981).

[17] S. Liu, C. E. Dykstra, K. Kolenbrander, and J. M. Lisy, J. Chem. Phys. **85**, 2077 (1986).

[18] Z. Latajka and S. Scheiner, J. Chem. Phys. **84**, 341 (1986).

[19] C. E. Dykstra, "Symposium on Clusters: Structures, Properties, and Dynamics," American Chemical Society National Meeting, Miami, FL, Sept. 12–16, 1989.

[20] D. D. Nelson, Jr. and W. Klemperer, J. Chem. Phys. **87**, 139 (1987).

[21] M. J. Howard, S. Burdensky, C. F. Giese, and W. R. Gentry, J. Phys. Chem. **79**, 192 (1983).

[22] B. Heijmen, A. Bizzari, S. Stolte, and J. Reuss, Chem. Phys. **126**, 201 (1988).

[23] F. Huisken and Th. Pertsch, Chem. Phys. **126**, 213 (1988).

[24] K. B. Laughlin, G. A. Blake, R. C. Cohen, D. C. Hovde, and R. J. Saykally, Philos. Trans. R. Soc. London Ser. A **324**, 109 (1988).

[25] G. A. Blake, K. B. Laughlin, R. C. Cohen, K. L. Busarow, D-H. Gwo, C. A. Schmuttenmaer, D. W. Steyert, and R. J. Saykally, Rev. Sci. Instrum. (in press).

[26] G. A. Blake, K. B. Laughlin, R. C. Cohen, K. L. Busarow, D-H. Gwo, C. A. Schmuttenmaer, D. W. Steyert, and R. J. Saykally, Rev. Sci. Instrum. (in press).

[27] K. L. Busarow, G. A. Blake, K. B. Laughlin, R. C. Cohen, Y. T. Lee, and R. J. Saykally, J. Chem. Phys. **89**, 1268 (1988).

[28] D-H. Gwo, M. Havenith, K. L. Busarow, R. C. Cohen, C. A. Schmuttenmaer, and R. J. Saykally, Mol. Phys. **71**, 453 (1990).

[29] D. D. Nelson, Jr., G. T. Fraser, K. I. Petersen, K. Zhao, W. Klemperer, F. J. Lovas, and R. D. Suenram, J. Chem. Phys. **85**, 5512 (1986).

[30] B. Heijman, A. Bizzari, S. Stolte, and J. Reuss, Z. Phys. D **10**, 291 (1988).

[31] J. T. Hougen and N. Ohashi, J. Mol. Spectrosc. **109**, 134 (1985).

[32] L. H. Coudert and J. T. Hougen, J. Mol. Spectrosc. **130**, 86 (1988).

[33] G. T. Fraser, R. D. Suenram, and L. H. Coudert, J. Chem. Phys. **90**, 6077 (1989).

[34] J. T. Hougen and L. H. Coudert, 44th Symposium on Molecular Spectroscopy, Ohio State University (1989).

[35] Calfit, is available through the NASA COSMIC program.

[36] M. J. Frisch, J. E. Del Bene, J. S. Binkley, and H. F. Schaefer, J. Chem. Phys. **82**, 2279 (1986).